Synthesis of $NiCo_2S_4$ Nanomaterial and its Composite for Electrochemical Energy Storage Devices

A thesis submitted towards the partial fulfilment of BS-MS programme

by

DEVENDRA SINGH
20141049

Under the guidance of

Dr. MANJUSHA V SHELKE

Senior Scientist
Physical & Material Chemistry Department CSIR-NCL,
Pune-411008

CERTIFICATE

This is to certify that this dissertation entitled **"Development of $NiCo_2O_4$/$NiCo_2S_4$ material and its composite with carbon for Electrochemical Energy Storage Devices"** towards the partial fulfilment of the BS-MS dual degree programme at the Indian Institute of Science Education & Research, Pune represents project carried out by **"DEVENDRA SINGH** at CSIR-NCL Faculty" under the supervision of **"Dr.Manjusha V. Shelke**, Sr. Scientist, Physical & Material's Chemistry Division" during the academic year 2018-2019.

Signature of Student

Signature of Supervisor

Date:

Place: Pune

DECLERATION

I hereby declare that the matter embodied in the report entitled "**Development of $NiCo_2O_4$/$NiCo_2S_4$ material and its composite with carbon for Electrochemical Energy Storage Devices**" are the outcomes of the work carried out at the Department of Physical and Materials Chemistry, CSIR-NCL Faculty, under the supervision of **Dr.Manjusha V. Shelke** and the same has not been submitted elsewhere for any other degree.

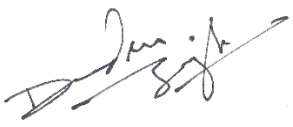

Signature of Student

Signature of Supervisor

Date:

Place: Pune

ACKNOWLEDGEMENT

With extraordinary joy here I am offering my thanks to all who were a part of my 10 months life in NCL. I might want to express gratitude toward Dr Ashwini Kumar Nangia, the honourable director of National Chemical Laboratory Pune and Dr P.A Joy, the head of Physical and Material Chemistry division, for giving me the open door for completing my Master's Thesis Project at CSIR-National Chemical Laboratory Pune.

I might want to offer my enormous thanks to Dr Manjusha V Shelke, my project guide to acknowledge me as her intern and for her incredible direction. My exceptional much gratitude goes to former Director of IISER-Pune Prof K. N. Ganesh and new director Prof Jayant B. Udgaonkar for giving a chance to completing this exploration work.

I am appreciative to Vikash, for directing and reproving me during the time. However grateful for his astounding and master guidance all through my MS Thesis. His understanding and productive exchanges were the preeminent help in the 10 months of project work in NCL. I wish to give true gratitude to Pravin, Golu, Swati, Ashvini, Rupali, Thripura, Poonam, Bhaskar, Indrapal, Nilesh, Varad, Amrutha and Swetha for giving me magnificent lab days and help. Additionally, I'd like to thank every one of my companions, Vamshi Krishna, Sunil Chaudhary, Rajat Patel, Naman Kalra, Yogesh Mahor, Satendra Birana, Harsha Gouda, Deepraj Pandit, Nenavath Parvathalu for all the annoyance we have done in college and making this adventure an important one.

DEVENDRA SINGH

TABLE OF CONTENTS

LISTING OF FIGURES vii

ABSTRACT 1

1. INTRODUCTION 2

1.1 Capacitors

1.2 Supercapacitors

1.3 Materials used for Supercapacitors

2. MATERIAL & METHODS 14

2.1 Experimental Section - I

2.1.1 Material and Reagent

2.1.2 Chemical Synthesis for Graphene Oxide

2.2 Experimental Section - II

2.2.1 Chemical synthesis for Nickel Cobalt Oxides (NCO)

2.2.2 Chemical synthesis for Nickel Cobalt Sulphide (NCS-1)

2.2.3 Chemical synthesis for Nickel Cobalt Sulphide (NCS) - DI

2.2.4 Chemical synthesis for Nickel Cobalt Sulphide (NCS) - EG

2.2.5 Chemical synthesis for a composite of rGO/Nickel Cobalt Sulphide

2.3 Characterization techniques

2.3.1 Preparation of working electrodes for electrochemical characterization

2.3.2 Cyclic voltammetry (CV)

2.3.3 Galvanostatic charge-discharge (GCD)

2.3.4 Electrochemical impedance spectroscopy (EIS)

3. RESULT AND DISCUSSION 19

3.1 Graphene Oxide

3.1.1 Material Characterisation

3.1.2 Electrochemical Characterization

3.2 Nickel Cobalt Oxides
3.2.1 Material Characterisation
3.2.2 Electrochemical Characterization

3.3 Nickel Cobalt Sulphide (via NCO-1 as precursor)
3.3.1 Material Characterization
3.3.2 Electrochemical Characterization

3.4 Nickel Cobalt Sulphide (DI water)
3.4.1 Material Characterization
3.4.2 Electrochemical Characterization

3.5 Nickel Cobalt Sulphide (EG)
3.5.1 Material Characterization
3.5.2 Electrochemical Characterization

3.6 rGO/Nickel Cobalt Sulphide (rGO/NCS)
3.6.1 Material Characterization
3.6.2 Electrochemical Characterization

4. CONCLUSION 36

5. REFRENCES 37

LIST OF FIGURES

1. INTRODUCTION

Figure1.1 Simplified scheme of a conventional capacitor 11

Figure1.2 Simplified diagram of (a) an electric double-layer capacitor (EDLC) and (b) a Pseudocapacitor (PC) 12

Figure1.3 Simplified diagrams of the various pseudocapacitance processes 13

2. METHODS AND MATERIALS

Figure2.1 Scheme of Cyclic voltammogram 20

3. RESULT AND DISCUSSION

Figure3.1 (a) XRD marking of Graphene oxide and
(b) TEM images of GO..... 22

Figure3.2 Graphene Oxide curves (a) CV curve with several scan rates,
(b) Charge-Discharge curves with several current densities
(c) Rate Capability scatter plot and (d) Nyquist graph.....23

Figure3.3 XRD marking of Nickel Cobalt Oxide r_1 & r_2.....24

Figure3.4 CV curve at several scan rate (a) NCO-r_1 and (c) NCO-r_2
& Galvanostatic Charge-Discharge (GCD) curves at various several current densities (b) NCO-r_1 and (d) NCO-r_2.....26

Figure3.5 NCO-r_1 and NCO-r_2 graphs for (a) Rate Capability scatter plot and
(b) Nyquist graph 26

Figure3.6 CV curves of NCO-r_1 and NCO-r_2 at scan rate of 10mVs..... 27

Figure3.7 XRD marking of NCS-1..... 28

Figure 3.8TEM image of NCS-1 at (a) 50nm and (b) 20nm..... 28

Figure3.9 NCS-1 curves (a) CV curve at several scan rates
(b) GCD curves at several current densities
(c) Rate Capability scatter plot and (d) Nyquist graph..... 29

Figure3.10 CV curves of NCS-1 and NCO-1 at scan rate of 10mVs..... 30

Figure3.11 (a) XRD pattern of NCS-DI and (b) TEM images of NCS-DI at 20nm 31

Figure3.12 NCS-DI curves (a) CV curve at several scan rate

(b) GCD at several current densities
(c) Rate Capability scatter plot and (d) Nyquist graph.....32
Figure3.13 CV curves of NCS-DI and NCS-1 at scan rate of 10mVs 33
Figure3.14 XRD marking of NCS-EG.....33
Figure3.15 SEM images of NCS-EG at several scale… 34
Figure3.16 NCS-EG curves (a) CV curve at several scan rates
(b) GCD curves at several current densities
(c) Rate Capability scatter plot and (d) Nyquist graph 35
Figure3.17 CV curves of NCS-EG and NCS-DI at scan rate of 10mVs 35
Figure3.18 SEM images of rGO/NCS 36
Figure3.19 rGO/NCS curves (a) CV curve at several scan rates
(b) Charge-Discharge curves at several current densities
(c) Rate Capability scatter plot and (d) Nyquist graph.....37

Abstract

Supercapacitor (SCs) and Li-ion based batteries (LiBs) are the two commercially mass successful systems for electrochemical energy storage. SCs have high power density while LiBs have high energy density. Their hybrid also used for better energy and power density combined. The material scientists have paid enormous attention to developing the different electrode materials for these systems resulting in the vast commercial success of energy storage devices. Carbon-based material as graphene, used as an electrode for SCs. The carbon materials are known for the highly stable electrode, but their disadvantage is their low theoretical capacity. Transition metal oxides (TMOs) electrodes store the charge through the faradaic process by conversion of the electron during charge-discharge. TMOs have a high theoretical capacity, but due to mass transfer and volume expansion, their cyclic stability is poor.

Here, we propose to develop $NiCo_2S_4$ electrode materials with the objective to address the challenge related to cyclic stability and storage capacity. We are planning to synthesize some $NiCo_2S_4$ by different synthesis procedure and further, their composites with the graphene, to achieve high capacity as well as high cyclic stability for electrochemical energy storage.

1. Introduction

Even in our new mobile phones, it seems there is never enough storage it turns out it's also true of energy, particularly for sustainable energy [1]. Nowadays, our present energy use relies on underground reservoir of natural gas, fuels and even water stored in dams for hydroelectricity. As our energy utilization changes, so will our energy storages selections. We may have to think in a different direction not just for energy storage but also for storing by-products of energy production such as carbon and carbon dioxide and when it comes to carbon we have to first capture before store it. Carbon dioxide is not only one that is causing environmental issues, black carbon also. Thus we have to look at a potential green solution [1]. The problem is renewable energy is unpredictable and it is difficult to store. Almost all the energy that we could generated from the renewable source is wasted or is not used effectively, for example in India (Tamil Nadu region), they have estimated that about half of the electricity that have been produced by wind power is lost. Thus the availability of natural processes [2], i.e., fossil fuels are limited, wind power and solar power availability, we need to come up with a promising solution with lesser drawbacks and cost efficiency to be in the technology race. Currently, the vast majority of electricity storage is provided by batteries and supercapacitor technologies [3] has developed altogether in the course of the most recent decade and rose with the possibility to encourage real advances in energy storage.

The battery is fundamentally a energy storage gadget which changes over it into electricalenergy just when it required. Primary battery and the secondary battery are two different categories of the battery. The primary battery is the non-chargeable while secondary battery is chargeable[4, 5]. Examples for primary batteries are the zinc-carbon and alkaline battery. Lithium-ion battery (LiBs), Nickel metal hydride (NiMH) battery and lead corrosive battery are models for secondary batteries.

Battery depends on the chemical reaction which implies for a lithium-ion battery to discharge energy when we need to wait the lithium will rearrange through an electrolyte and when we need to store energy, wait for lithium will rearrange back. Lithium-ion battery additionally corrodes, and repalcing one out of an electric vehicle would be gigantically costly. Conversely, Capacitor store electricity produced via friction like what develop what based on an inflatable balloon as you rub it on your

hair. On the off chance that research and exploration is precise we would one be able to face a daily reality such that automobiles can be completely charged in the minutes rather than hours and their capacity storage units would a decades ago rather than years.

1.1 Capacitors

Capacitors utilize friction based electricity (electrostatics) instead of science to store energy. Conventional capacitors comprise of two conduction plates isolated by a protecting material called dielectric. At the point when a potential is connected to a plate, inverse charges amass on the surfaces of each plate. The charges are kept separate by the dielectric, consequently creating an electric field that enables the capacitor to store energy [6].

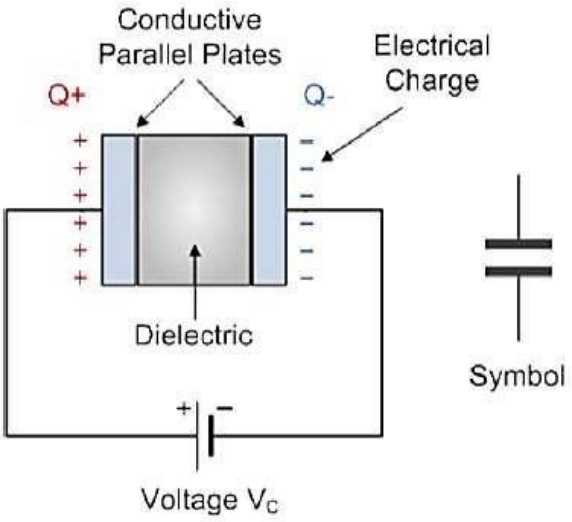

Figure1.1 Simplified scheme of a conventional capacitor
https://www.researchgate.net/profile/Ahmed_Tarek12/publication/305115547/figure/fig4/AS:382402481410053@1468183264449/Figure-4-basic-structure-of-capacitor.png

Capacitance C is characterized as the proportion of stored (positive) charge Q to the connected voltage V:

$$C = \frac{Q}{V}$$

For a conventional capacitor, C is directly relative to the surface region A of each plate and conversely corresponding to the separation D between the plates:

$$C = \varepsilon_0 \varepsilon_r \frac{A}{D}$$

Whereas, ε_0 is the permitivity of free space and

ε_r is the dielectric constant of the material between plates

The energy E stored in a capacitor is directly related to its capacitance:

$$E = {}^{1}/_{2}\, CV^2$$

1.2 Supercapacitors

They are unique in relation to conventional capacitors by two different ways; its plates viably have a lot greater region and the separation between them is a lot littler, in fact that the separator between them works contrastingly to a regular dielectric. The conventional capacitors plates are isolated by a moderately thick dielectric produced using something like mica (a ceramic), a slim plastic film, or even basically air, but in a supercapacitor there is no dielectric. Rather, the two plates are absorbed an electrolyte and isolated by an extremely meagre protecting layer created at the anode electrolyte interface [6]. Therefore, electrochemical capacitors called Supercapacitors (SCs) are a sort of essential energy storage devices with higher energy density [4, 5] than conventional capacitors and high power density than batteries. Additionally, Supercapacitors have gotten incredible consideration because of its fast conveyance of energy, non-danger and longer life expectancy than batteries.

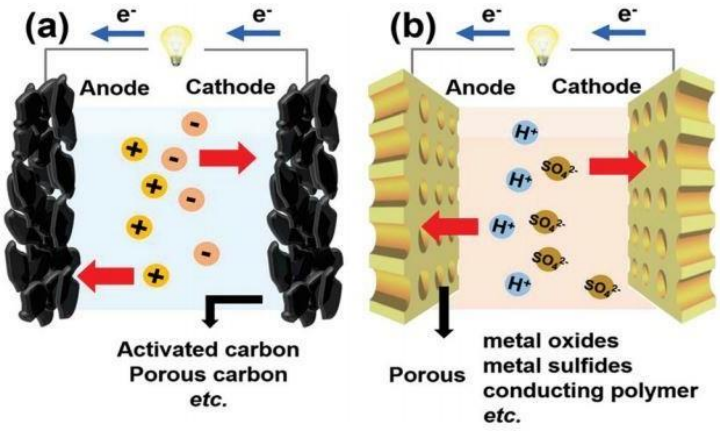

Figure1.2 Simplified diagram of (a) an electric double-layer capacitor (EDLC) and (b) a Pseudocapacitor (PC)

https://pubs.rsc.org/en/content/articlepdf/2016/nr/c6nr00796a/Fig.1

Supercapacitors have been categories as Pseudocapacitor (i.e., stores charge electrochemically) and Electrochemical Double layer capacitor (EDLC) (i.e., stores charge electrostatically).

For the working of a Pseudo capacitor three different mechanisms occurs: Under potential Deposition [7, 8], Redox pseudocapacitance[9, 10]and intercalation [11] pseudo capacitance. The total pseudo capacitance offered by a capacitor is contributed by these three different mechanisms. In Under Potential Deposition electrostatic surface charging occurs and the movement of ions is limited by the ionic conductivity of the electrolyte. Charge accumulation at the surface causes a reduction in capacity and leads to lower energy density. It possesses good cycle stability due to the absence of electrode degradation by redox reactions. The material which is able to show different or multiple oxidation states within the operating voltage window of the electrolyte chosen as redox reactions occur and it exhibits greater capacity due to the electron transfer across the electrode-electrolyte interface.

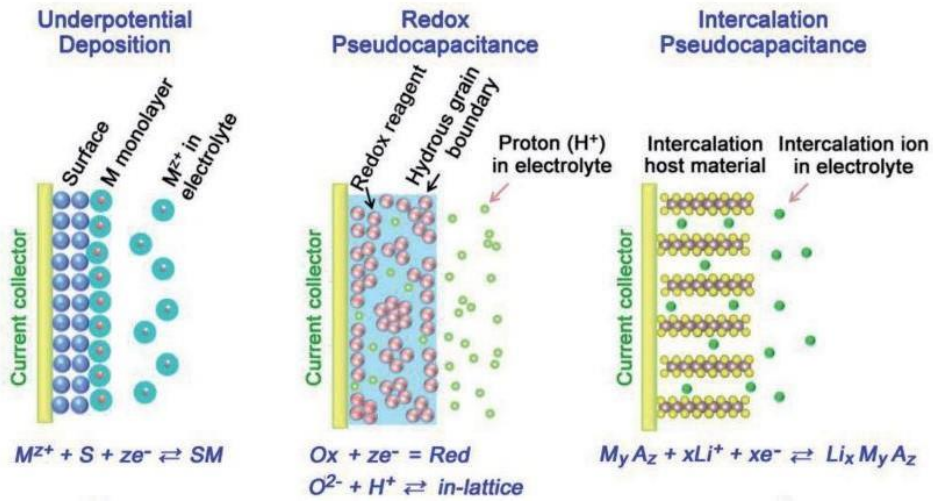

Figure1.3 Simplified diagrams of the various pseudocapacitance processes https://onlinelibrary.wiley.com/doi/pdf/10.1002/advs.201700322/Figure4.

The third mechanism is intercalation and in this cations are diffused deeper into the electrode framework which allows more of them to diffuse resulting in a large amount of charge stored. According to the diffusion length of cations, the efficiency can change in them. Diffusion length is determined by the electrode arrangement. Smaller the diffusion length faster will be the process. Nanostructures helps in

reducing the diffusion length [12] and hence speed up the charge intake. This mechanism is relatively slow in occurrence because ions have to cover a distance to get diffused and also due to the higher resistance encountered in an electrode structure. As a Consequence of this, the charge/discharge rates get lower [12]. The first two mechanisms occur at the surface and ensure a fast charge/discharge rate.

1.3 Materials used for Supercapacitors

There have been broad investigations of assortments of Carbon based materials for supercapacitor as a result of their extensive specific surface area (SSA), high conductivity, easy accessibility, and compound stability [13, 14]. Some of best Carbon-based material are Carbon Nanotubes (CNT) [15], fullerene, Graphene [16, 17], reduced Graphene oxide, activated carbon [18], etc. utilized as an electrode for SCs. The carbon materials are known for the profoundly steady electrode; however, their disadvantage is low theoretical capacity [13-17]. **Graphene** is the thinnest material we can envision it's only one atomic thick. Graphene is anything but a one of a kind or uncommon substance; it has a similar carbon structure as graphite which we utilize each day for outlining and composing. About just 3'' inches of graphite comprises of 3 million layers of the Graphene sheet. Graphene is unimaginably stretchy it can extend as much as one fourth of its original length. This material is additionally hardened; it's the hardest material individuals know considerably harder than the precious stone. In spite of being 2-D it can impeccably obvious to bare eyes. One more noteworthy thing about Graphene is a connection with power and electricity, this material conveys electricity more rapidly, more accurately and more productively than other known material [16, 17]. The reason is that the current density of Graphene is many million times better than that of copper. Its intrinsic mobility is much better than silicon also. Thus electrons have no resistance when they move through Graphene as a result Graphene can be potentially used to produce batteries and make composites with active material in Pseudo capacitor that will have 10 times the electrical capacity retention. Interestingly Graphene can expand when cooled and strength when it gets warm, there are no other examples of materials with similar quality. Since all normal substance acts in the opposite way, they become larger when they are heated and smaller when they get cold. Graphene is the most impermeable material discovered so far. Graphene can be used in many ways like in

body armour, make ocean water drinkable, it can assist in detecting cancerous cells in the body and used in making flexible smart phones displays [16, 17].

Transition metal oxides (TMOs) electrodes store the charge through the faradaic process by conversion of the electron during charge-discharge. Transition Metal Oxides/ sulphides have a high theoretical capacity, but due to mass transfer and volume expansion, their cyclic stability is poor. As of late, change metal sulphides have pulled in incredible consideration on account of their superb properties and promising applications in electronic, optical and optoelectronic gadgets [15-19]. The performance of LIBs and SCs depends on the electrode material applied and also their properties can be improved by some modifications in the active material. Transition metal oxides, hydroxides and sulphides of the type RuO_2, MnO_2, NiO, Co_3O_4, $Co(OH)_2$, $Ni(OH)_2$, $NiCo_2O_4$, $NiCo_2S_4$ and so on with high specific capacitance are used as the electrode material [24-27]. In recent times ruthenium oxide (RuO_2) is the commonly used anode material [28, 29] for Pseudocapacitor but it is toxic and expensive. Studies revealed that among the various transition metal oxides cobalt oxides shows desirable anodic properties. But due to toxicity and high expense of cobalt Co_3O_4 is partially replacing by friendly alternatives like nickel oxide (NiO). While considering cost-efficiency, resource abundance, good corrosion stability and environmental friendliness oxides of nickel and cobalt are more appropriate. NiO has certain properties like reasonable pore measure, extensive specific surface zone, high capacity and energy density [30] but there are some disadvantages like high resistivity and poor cycle stability which makes its use restricted. $NiCo_2O_4$, $ZnCo_2O_4$, $CuCo_2O_4$, $MnCo_2O_4$[31, 32] etc. are the ternary metal oxides suggested and among them, $NiCo_2O_4$ which is a combination of NiO with Co_3O_4 or CoO is considered as the one of the most promising electrode material. $NiCo_2O_4$ has high electronic conductivity and electrochemical activity arising from the combined effect of metal ions and rich redox sites. Ternary metal sulphides ($NiCo_2S_4$) [33-36] shows better performance than ternary metal oxides [37, 38]. In the same sense, ternary metal sulphides show good capacitance than their individual metal sulphides.

Conducting polymers(CP) -based materials shows high potential in supercapacitors because of their unique advantages including good conductivity, flexibility, relatively cheap, easy of synthesis and so on. Materials which shows

promising capacitance is polypyrrole (PPy), polyaniline (PANI), and polythiophene (PTh) [39, 40].

By investigating all the types of supercapacitors have shown some disadvantages for applications, such as low specific capacitance in carbon-based materials, low conductivity in transition metal oxides, and poor cycling stability in conducting polymers.

In this work, we have first synthesised Graphene oxide from modified hummers method and also synthesised $NiCo_2O_4$ and $NiCo_2S_4$ by severalmethods i.e. hydrothermal, solvothermal or reflux method. By using the synthesized Graphene Oxide, $NiCo_2O_4$ and $NiCo_2S_4$ materials, we have also fabricated EDLC and Pseudocapacitor electrode respectively with enhanced electrochemical performances. Graphene can on a basic level accomplish EDLC of 21 mF/cm^2 [41], and with the total surface zone, an EDLC of Graphene could reach as high as 550 F/g (theoretically set) alongside high energy density, high power density, and long term dependability [41]. $NiCo_2O_4$ and $NiCo_2S_4$ are known as outstanding electrode materials for SCs. Structural characteristics like porosity, uniformity of the surface composition, etc. intensify the electrochemical actions of $NiCo_2O_4$ and $NiCo_2S_4$. Presence of mesoporous in the system gives great electrolyte diffusion and expansive electrode electrolyte contact region, and furthermore the volume change during charge/release process is adjusted by this structure. By adjusting the morphologies, we can obtain SCs with varying electrochemical performance. The studies on the morphologies of $NiCo_2O_4$ and $NiCo_2S_4$ revealed that the hierarchical mesoporous structure exhibit greater electrochemical performance. Among various dimensions of the materials, due to reduced ionic diffusion pathway in one-dimensional material, it shows high performance than two dimensional and three-dimensional materials. So as to accomplish greatest capacitance, porous materials can be utilized because of their high specific surface area and little crystal volume and size [37-41]. After all combination we made the composites of both materials since significant favourable advantage is that the maintenance of capacitance alongside long cyclic life.

2. Materials and Methods

2.1 Experimental Section

2.1.1 Material and reagent

Graphite flakes (Sigma-Aldrich), Sodium Nitrate (Thomas Baker), Hydrochloric Acid (Thomas Baker), Potassium permanganate (Alfa Aesar), Hydrogen peroxide (30% by Thomas Baker), Sulphuric Acid (Thomas Baker), PTFE membrane (Sartorius Stedim Biotech), Acetone, Ethanol, no further purification of material or reagent is done in synthesis part.

2.1.1 Chemical synthesis of Graphene Oxide

It includes both oxidation and shedding of graphite sheets.

2g of Graphite flakes and 2g $NaNO_3$ were dissolved down in 90 mL of H_2SO_4(98%) in a 500 ml volumetric flask with consistent blending. 4 hrs of mixing and included 12g of $KMnO_4$ to the suspension in all respects gradually. Deliberately controlled the response temperature lower than 15º C. The mixture is diluting with the 184 ml of water and mixed for 2 hrs. The ice shower was evacuated, and the mixture is mixed at 35°C for 2 hrs. Place response in a reflux framework at 98°C for 10-15 min. In the wake of changing the temperature to 30°C dark coloured compound acquired. After 10 min, swing it to 25°C and keep up it for 2 hrs. Treated with 40 ml H_2O_2 gives the last yellow shading solution. 100 ml of water taken in two separate measuring cylinders and an equivalent measure of arrangement arranged is included and stirred for one hr. It kept without stirring for 3-4 hrs, where the particles settle at the base, and the rest of the water is poured to channel. The subsequent solution is washed over and over by centrifugation with 10% HCl and after that with deionized (DI) water a few times until it progresses toward becoming structures gel-like substance (pH-neutral). After centrifugation, the gel-like material is vacuum dried at 60°C for in excess of 6 hrs to GO powder.

2.2 Material and reagent

Nickel Nitrate hexahydrate ($Ni(NO_3)_2.6H_2O$), Cobalt acetate tetrahydrate ($Co(CH_3COO)_2.4H_2O$), Cobalt Nitrate hexahydrate ($Co(NO_3)_2.6H_2O$) Nickel acetate tetrahydrate ($Ni(CH_3COO)_2.4H_2O$), Ethylene glycol ($(CH_2OH)_2$), Urea ($CO(NH_2)_2$), Thiourea ($SC(NH_2)_2$), Sodium Sulfide nonahydrate (Na2S.9H2O) are synthetic

chemicals are obtained from Sigma-Aldrich from India. Furthermore, is utilized with no further refinement.

2.2.1 Chemical synthesis of Nickel Cobalt Oxides (NCO)

NCO was prepared by a facile hydrothermal process. 0.8739g of $Co(NO_3)_2.6H_2O$ and 0.4351g of $Ni(NO_3)_2 .6H_2O$ were dissolved in 40mL of deionized water and 40mL of Ethylene Glycol under the conditions of continuous stirring for 30 min to form a transparent pink solution. To this solution, 0.816g of urea was added and stirred for 1 hour and checked pH. Then, it was transferred to a 100mL Teflon lined stainless steel autoclave. It was heated at 160^oC for 12hours at two different ramp rates named NCO-r_1 and NCO-r_2. In the wake of cooling the autoclave to room temperature, the acquired item was separated and washed a few times with DI water and ethanol until it winds up neutral. It was kept for drying medium-term at 80^oC. The got precursor was annealed at 450^oC for 5hours.

2.2.2 Chemical synthesis of Nickel Cobalt Sulphide (NCS)

0.2g of above-obtained precursor (NCO-r_1) and 0.6g of $Na_2S.9H_2O$ dissolved in 20mL of DI water under continuous magnetic stirring. Then, the solution transferred to a 25mL Teflon lined steel autoclave. It was heated for 180^oC for 12 hours. After cooling the autoclave to room temperature, the acquired product was washed several times with DI water and ethanol until it became neutral and kept overnight at 80^oC for drying.

2.2.3 Chemical synthesis of Nickel Cobalt Sulphide (NCS) - DI (Hydrothermal)

NCS prepared by a facile hydrothermal method. 0.498g of $Co(CH_3COO)_2.4H_2O$ and 0.248gof $Ni(CH_3COO)_2.4H_2O$ dissolved in 30mL of DI water under the conditions of continuous stirring for 30 min. To this solution, 0.1148g of thiourea was added and stirred for 1 hour and checked pH. Then, it transferred to a 100mL Teflon lined stainless steel autoclave. It heated at 180^oC for 24hours. In the wake of cooling the autoclave to room temperature, the acquired item was separated and washed a few times with DI water and ethanol until it winds up neutral and kept for drying in overnight.

2.2.4 Chemical synthesis of Nickel Cobalt Sulphide (NCS) - EG (Solvothermal)

NCS prepared by a superficial solvothermal method. 0.498g of $Co(CH_3COO)_2.4H_2O$ and 0.248gof $Ni(CH_3COO)_2.4H_2O$ dissolved in 30mL of Ethylene glycol under the conditions of continuous stirring for 30 min. To this solution, 0.1148g of thiourea was added and stirred for 1 hour and checked pH. Then, it transferred to a 100mL Teflon lined stainless steel autoclave. It heated at 180^oC for 24hours. In the wake of cooling the autoclave to room temperature, the acquired item was separated and washed a few times with DI water and ethanol until it winds up neutral and kept for drying in overnight.

2.2.5 Chemical synthesis of a composite of rGO/Nickel Cobalt Sulphide (NCS)

20 mg of the prepared graphite oxide was scattered in 60 ml of ethylene glycol (EG) through ultra-sonication to frame a homogeneous graphene oxide (GO) suspension. (0.5mmol) of Ni(Ac)2.4H2O and (1mmol) of Co(Ac)2.4H2O were included into the above suspension step by step, and after that the mixture was mixed at 80 °C for 2 h. Thusly, 6 mmol of thiourea was brought into the above suspension arrangement. The resultant stirred was continued mixing for 2h and after that was refluxed at 180 °C for 3 hrs. In the wake of cooling the autoclave to room temperature, the acquired item was separated and washed a few times with DI water and ethanol until it winds up neutral and kept for drying in overnight at 80^oC

2.3 Characterization techniques

2.3.1 Preparation of working electrodes for electrochemical characterization

Working electrodes, for electrochemical studies, were prepared by taking 80:15:5 as of synthesized material, carbon black, and PVDF (a binder) respectively using N-methyl-2- pyrrolidinone (NMP) as a solvent. Uniform slurry was prepared by grinding the above mixture and then it was coated ($1cm^2$*$1cm^2$) onto a Toray Carbon electrode. The Toray carbon paper was dried overnight in an oven at 100^oC before and after coating for testing. The electrochemical measurements were conducted in an essential medium using 3M KOH for Ternary metal oxides and sulphides and 1M H_2SO_4 for graphene supercapacitor as an electrolyte for CV, GCD, and EIS using a three electrode system and two electrode system for Pseudocapacitor and EDLC

respectively, where the Platinum electrode was used as a counter electrode with Ag/AgCl and Hg/HgO as a reference electrode.

2.3.2 Cyclic voltammetry (CV)

Cyclic voltammetry is the most regularly utilized system for considering electrochemical response mechanism i.e., redox reaction mechanisms occurring in electrochemical analysis. In a cyclic voltammetry experiment, the working electrode is scanned linearly from an initial applied voltage E_1 to a final switching voltage E_2 at which the direction of the scan is reversed. The connected voltage is known as the sweep rate which implies that during the experiment the potential differs directly at that speed. The current is plotted as a function of connected voltage. The crests in a CV graph speaks to redox forms.

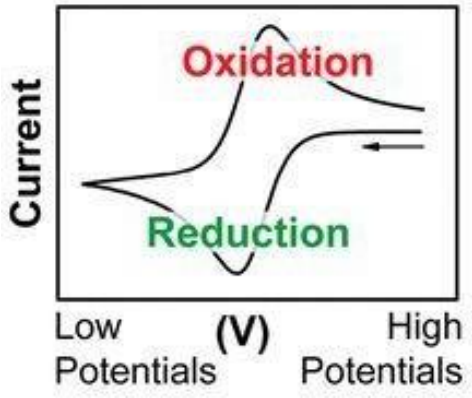

Figure2.1 Simple Scheme of Cyclic voltammogram curve

During the negative sweep the analyte experiences reduction, and the relating current is known as cathodic current same when the output is a positive way, the oxidation of the analyte happens, and the current comparing to the oxidation peak is called anodic current. The particular capacitance from CV is determined by the given equation

$$C = \frac{\int I \,.\, \Delta v}{v.\, m.\, \Delta V}$$

whereas, $\int I$ denoted negative current swiped area by CV, ΔV is potential window , m is electroactive material mass, v is scan rate

In a three-electrode system, the potential is estimated between the working and reference electrode and the current is estimated between the working and counter electrode.

2.3.3 Galvanostatic charge-discharge (GCD)

Galvanostatic charge-discharge is an electrochemical technique conducted to measure the electrochemical performance and cycle life of batteries and capacitors. In this technique, the electrode is charged and discharged cyclically. For the analysis a constant current is applied between the working and reference electrode and the potential between the working and counter electrode concerning the reference electrode is measured. Both charging and discharging are conducted at constant current applied until a set voltage is reached. For data analysis, the potential of the electrode is plotted as a function of time concerning a reference electrode.

2.3.4 Electrochemical impedance spectroscopy (EIS)

Impedance can be defined as the measure of the ability of a circuit to resist the flow of electric current. Naturally, it is a tool for the analysis of non-linear electrochemical processes. In the EIStechnique, the measurements are made by applying a small sinusoidal potential of fixed frequency, and the response is obtained as a sum of sinusoidal functions. It is capable of delivering information about the diffusion resistance capacitive behaviour of the material and the rate of electron transfer reactions. The data obtained from an EIS technique are represented in a way that the real part is plotted along X-axis and the imaginary part along Y-axis, such plots are referred to as Nyquist plots, and each point present in them represents the impedance at that frequency.

3. Result and Discussion

3.1 Graphene Oxide (GO)

3.1.1 Material Characterisation

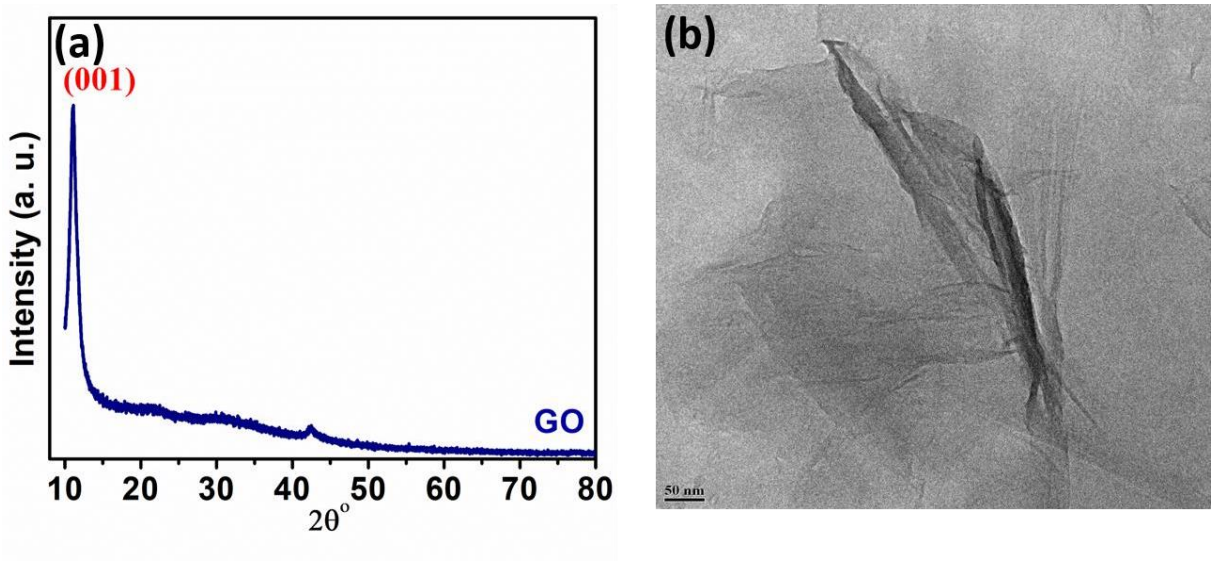

Figure 3.1(a) XRD marking of Graphene oxide and (b) TEM images of GO

The atomic structural composition of Graphene oxide is confirmed via XRD graph shown above in fig 3.1, in which a characteristic peak is evident at 2θ=10.3ºwhich is due to oxidation of graphite material and a peakcorresponding to (001) plane of the diffraction peak of ordered Graphene oxide. Usually, the diffraction peak for graphite is found at ~26º which correspond to (002) plane as a highly organized layer structure. As in fig 3.1, the disappearance of 26º and appearance of 10.3º shows complete oxidation of graphite. TEM image shows the sheets of graphene.

3.1.2 Electrochemical Characterization

The capacitive properties of the Graphene oxide are tested via two electrode system. In each investigation a symmetric plan is used, guaranteeing both counter and working electrode are of a similar piece. The electrodes are associated and submerged into the electrolyte of 1M H_2SO_4. The capacitive performance is assessed by methods for cyclic voltammetry and Galvanostatic charge and discharge cycle. And internal resistance test performed using electrochemical impedance spectroscopy. The system is fixed at 0 to 1V potential window for CV and GCD.

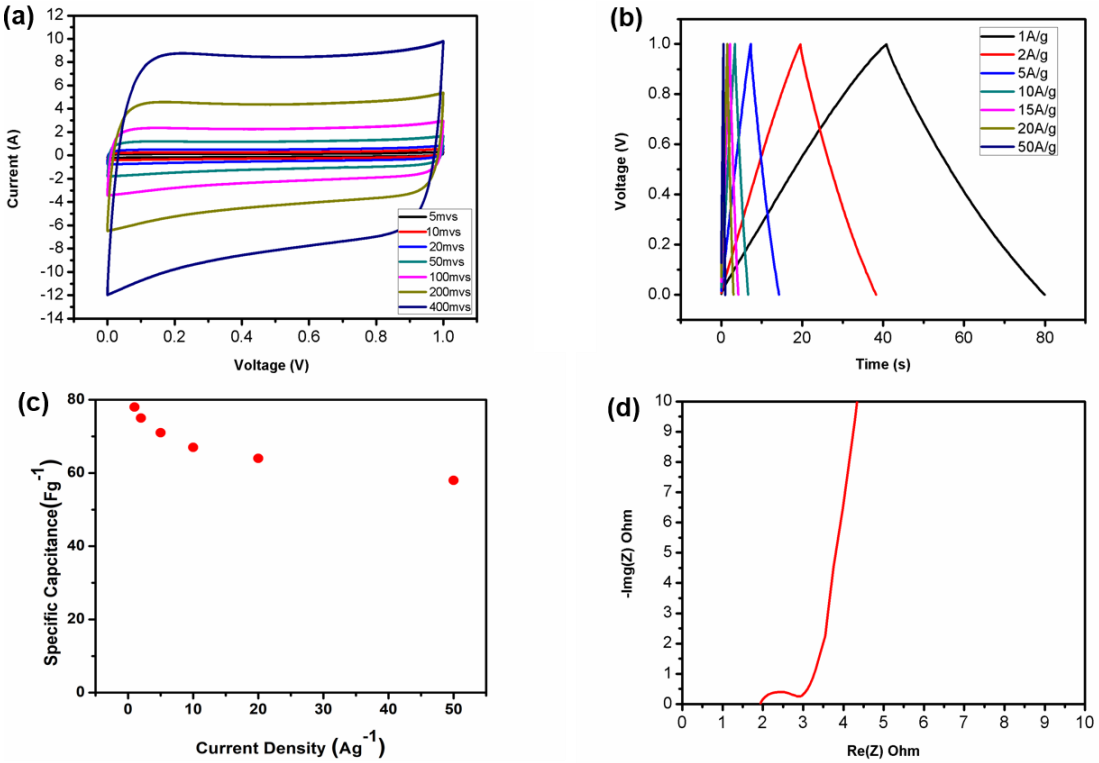

Figure3.2 Graphene oxide curves (a) CV curve at several scan rates (b) Charge-Discharge curves at several current densities (c) Rate Capability scatter plot (d) Nyquist graph

The CV curves from figure 3.2 at all sweep rates demonstrated very much characterized rectangular shape which approves the arrangement of a fine EDL interface between the active material and ions. As the scan rate increases the molecules find difficult to absorb compared to slow scan rate. The specific capacitance calculated from CD curve at 1A/g, 2A/g, 5A/g, 10A/g, 20A/g, 50A/g is 78F/g. 75.4F/g, 71.4F/g, 67.7F/g, 64.3F/g, 58.8F/g respectively. The sametrend follows in capacitance in the CD curve because of increasing current Density. CD curves show symmetric triangle curves demonstrating capacitance from EDL and high-charge portability at the electrode surface. In rate Capacity curve the retention of material is greater than 75% for 1A/g to 50 A/g.

To additionally comprehend the electrochemical performance qualities, we depended on electrochemical impedance spectroscopy (EIS) completed at open circuit potential in the recurrence scope of 100kHz to 50mHz. Figure 3.2 demonstrates the Nyquist plots. The EIS information were fitted dependent on a proportionate circuit

display comprising of bulk solution hindrance R_s, charge-transfer hindrance R_{ct}, double layer capacitance C_{dl}, and Warburg opposition (W), and the outcome is appeared in Figure 3.2. The EIS information uncover that the GO electrodes demonstrate a lot littler R_{ct} (0.28ω) in the Nyquist plots and internal resistance is 1.9ω.

3.2 Nickel Cobalt Oxides

3.2.1 Material Characterisation

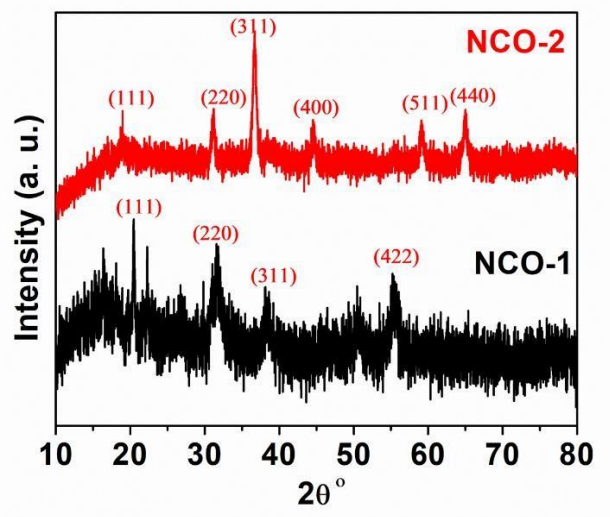

Figure3.3 XRD marking of Nickel Cobalt Oxide r_1 & r_2

Every one of the peaks (Fig. 3.3) of the example can be allotted to the reflection planes of the $NiCo_2O_4$ crystalline phase (JCPDs no.# 20-0781) which are ordered to (111), (220) and (311) planes at an edge 20.9°, 32.2°, 38.7° are showed up in the two synthesis. The planes (400), (511) and (440) at 44.7°, 58.5° and 64.3° show up in NCO-r2 test while (422) plane shows up at an edge 55.2º. Appearances of noteworthy peaks show the nearness of high purity $NiCo_2O_4$.

3.2.2 Electrochemical Characterization

The mass loading of active material for electrochemical characterisation is ~1mg.

The capacitive properties of the $NiCo_2O_4$ are tried through a three electrode configuration. In this trial an asymmetric arrangement of action is used, counter as Platinum anode and working cathode as Ag/AgCl. The anodes are associated and submerged into the electrolyte of 3M KOH. The capacitive performance is assessed by methods for cyclic voltammetry and Galvanostatic charge and release cycle. The

cyclic voltammetry estimations were directed at various output rates in a voltage window of 0-0.5 V for NCO-r_1 and 0-0.6V for NCO-r_2 and a similar window for GCD. In the CV curves. It is noticeable NCO-r_1 and NCO-r_2 haves one peak in oxidation and one peak in reduction because of the accompanying reaction:

$$\mathbf{NiCo2O4 + OH- + H2O \leftrightarrow NiOOH + 2CoOOH + 2e-}$$

$$\mathbf{CoOOH + OH- \leftrightarrow CoO2 + H2O + e-}$$

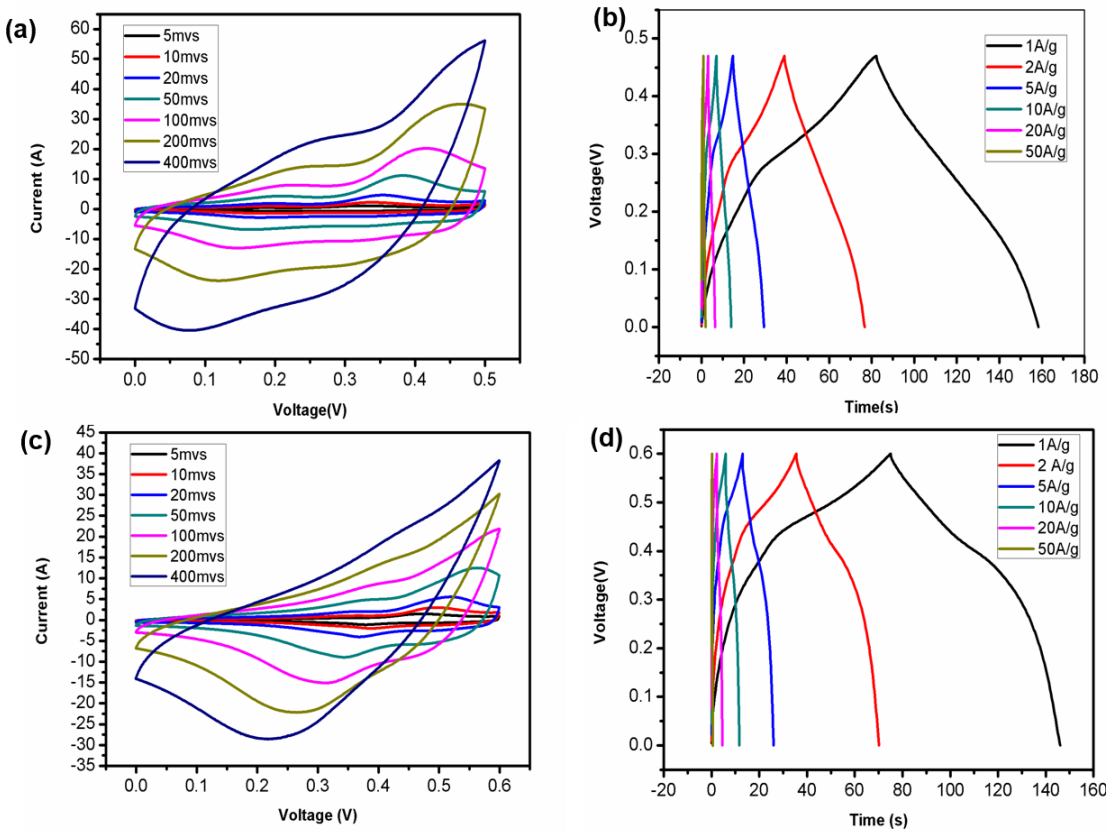

Figure 3.4 CV curve at several scan rates (a) NCO-r_1 and (c) NCO-r_2 & Galvanostatic Charge-Discharge (GCD) curves at several current densities (b) NCO-r_1 and (d) NCO-r_2

As the sweep rate builds oxidation and reduction peak moved towards progressively potential because of the dispersion rate of electrolyte (OH^-) particles at a high output rate isn't fast to for response of active material. Capacitance calculated from CD curve at 1A/g, 2A/g, 5A/g, 10 A/g, 20 A/g, and 50A/g is 206.3F/g. 203.8 F/g, 100 F/g, 178.8 F/g, 171.82 F/g and 144.8 F/g for NCO-1 and 120.11 F/g, 117.77 F/g, 108.02 F/g, 106.62 F/g, 94.24 F/g, 83.33 F/g respectively for NCO-2. The same trend

follows of decreasing specific capacitance in the CD curve because of increasing current density.

To additionally comprehend the electrochemical performance qualities, we depended on electrochemical impedance spectroscopy (EIS) completed at open circuit potential in the recurrence scope of 100kHz to 50mHz. Figure 3.2 demonstrates the Nyquist plots. The EIS information were fitted dependent on a proportionate circuit display comprising of bulk solution hindrance R_s, charge-transfer hindrance R_{ct}, double layer capacitance C_{dl}, and Warburg opposition (W), and the outcome is appeared in Figure 3.5

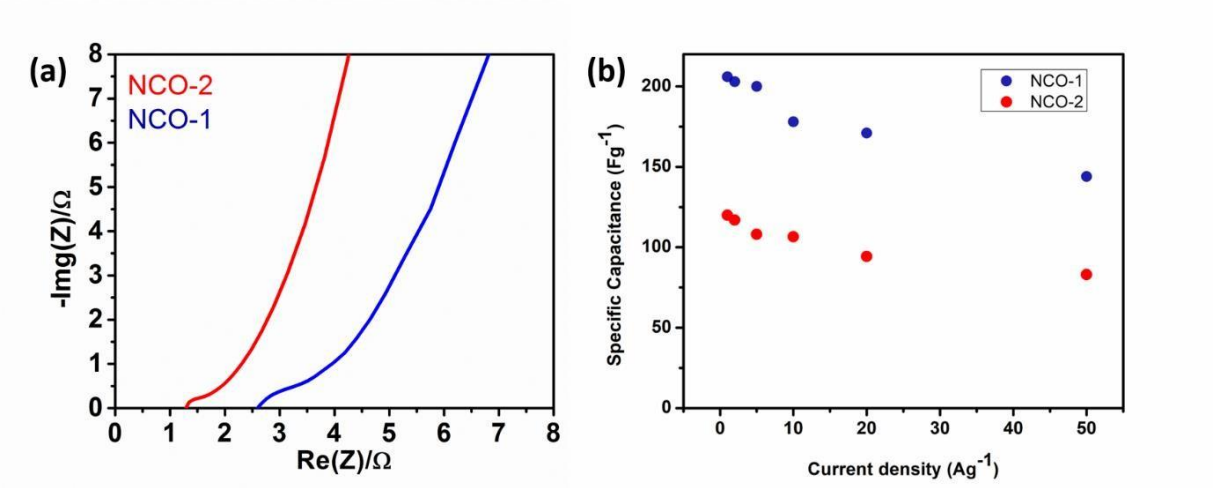

Figure 3.5 NCO-r_1 and NCO-r_2 graphs for (a) Nyquist graph and (b) Rate Capability scatter plot

The EIS information uncover that the NCO electrode demonstrate a little radius for charge transfer. Corresponding R_{ct1} and R_{ct2} are (0.31Ω) and (0.22Ω) in the Nyquist plots and internal resistance are 1.3Ω and 2.1Ω. In rate Capacity curve (fig 3.5) the retention of material is greater than 70% for both materials.

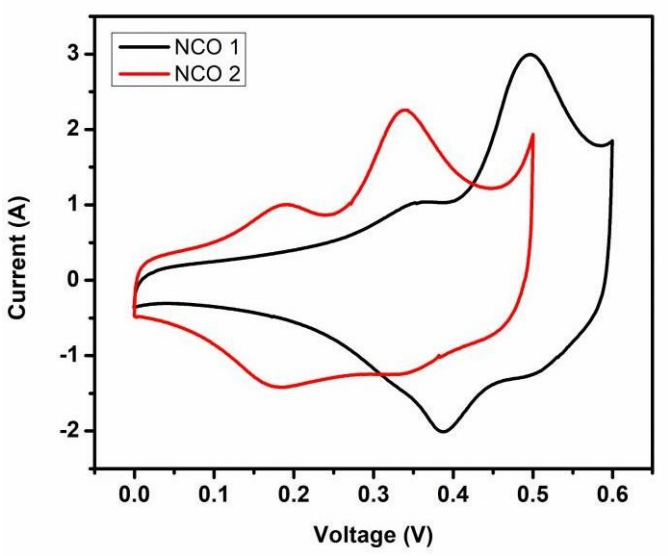

Figure 3.6 CV curves of NCO-r_1 and NCO-r_2 at scan rate of 10mVs

For the hydrothermal synthesis of $NiCo_2S_4$ (NCS-1) through NCO (as precursor) we selected NCO-r_1 as in Fig.3.6 we compared their CV curves at 10mVs and it is clearly noted the integral current for NCO-r_1 is greater than NCO-r_2. To obtain a good capacitance of NCS-r_1 we considered NCO-r_1 over NCO-r_2.

3.3 Nickel Cobalt Sulphide (NCS-1) (a NCO-1 as precursor)

3.3.1 Material Characterization

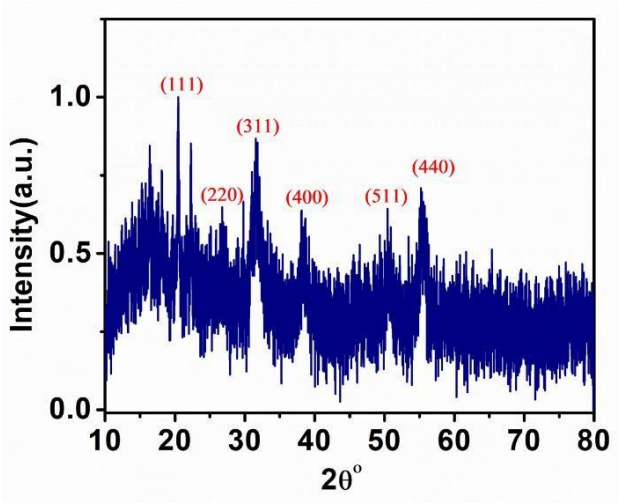

Figure3.7 XRD marking of NCS-1

The crystal phases of NCS-1 material were examined by XRD as shown in Figure 3.7. In reference with the JCPDS card number # 43-1477, the peaks indexed as

(111) (220), (311), (400), (511), (440) correspond to angles 21.8º, 26.7º, 31.6º, 38.4º, 50.5º and 55.3º respectively. It is not very evident in the background probably because of high diffraction intensities of NCS and background noise.

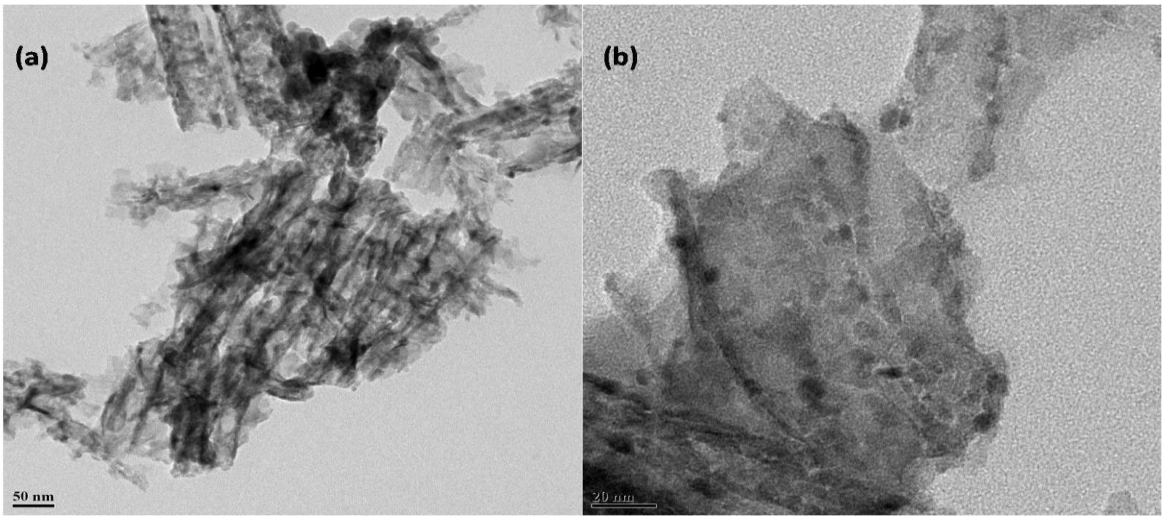

Figure 3.8 TEM image of NCS-1 at (a) 50nm and (b) 20nm

The TEM images of NCS-1 in fig.3.8 showed mixed nano-needle and sheet-like morphology. On closer analysis, it can be observed that small crystallites of NCS are taking the shape of needles or sheets in different regions during the hydrothermal treatment.

3.3.2 Electrochemical Characterization

The capacitive properties of the $NiCo_2S_4$ are tried through a three electrode configuration. In this trial an asymmetric arrangement of action is used, counter as Platinum anode and working cathode as Ag/AgCl. The anodes are associated and submerged into the electrolyte of 3M KOH. The capacitive performance is assessed by methods for cyclic voltammetry and Galvanostatic charge and release cycle. The cyclic voltammetry estimations were directed at various output rates in a voltage.

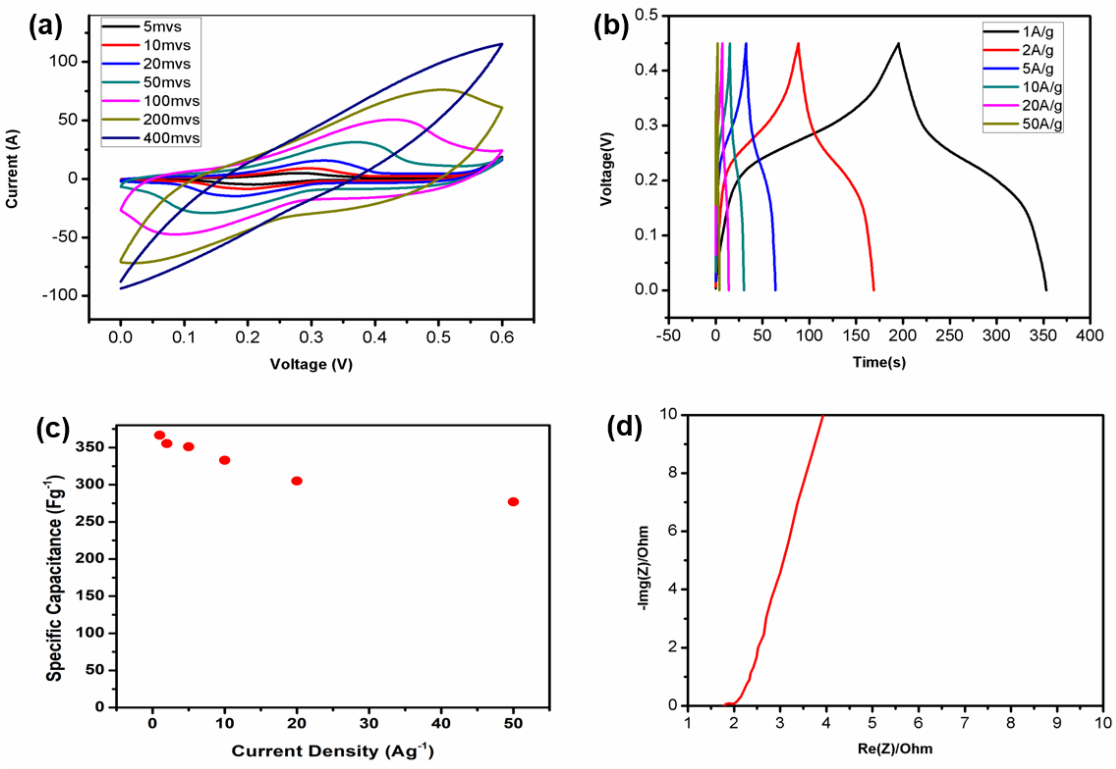

Figure3.9 NCS-1 curves (a) CV curve at several scan rates (b) Charge-Discharge curves at several current densities (c) Rate Capability scatter plot (d) Nyquist graph

The system is fixed at 0 to 0.6V potential window for CV and GCD. The cyclic voltammetric measurements were conducted at different scan rates. In CV curve it is visible it has one peak in oxidation and one peak in reduction due to the following reactions

$$\mathbf{NiCo2S4 + OH^- + H2O \leftrightarrow NiSOH + 2CoSOH + 2e^-}$$

$$\mathbf{CoSOH + OH- \leftrightarrow CoSO + H2O + e^-}$$

Capacitance calculated from CD curve at 1A/g, 2A/g, 5A/g, 10A/g, 20A/g and 50 A/g is 366.6F/g, 355.5F/g, 351.5F/g, 333.33F/g, 305.6F/g and 277F/g. The same trend follows of decreasing specific capacitance in the CD curve because of increasing current Density. In rate Capacity curve the retention of material is greater than 78%. To additionally comprehend the electrochemical performance qualities, we depended on electrochemical impedance spectroscopy (EIS) completed at open circuit potential in the recurrence scope of 100kHz to 50mHz. Figure 3.9 (d) demonstrates the Nyquist plots. The EIS information uncover that the NCO electrode demonstrate

a little radius for charge transfer R_{ct} (0.36Ω) in the Nyquist plots and internal resistance is 1.6Ω.

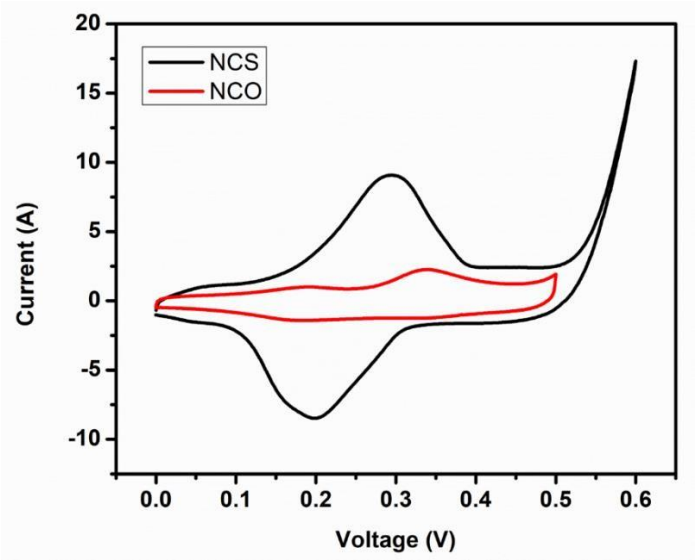

Figure 3.10 CV curves of NCS-1 over NCO-1 at scan rate of 10mVs

In comparison with the NCO-1 electrode, the NCS-1 electrodes exhibit large integral in CV curves (Fig. 3.10), indicating the NCS-1 electrodes possess higher specific capacitances. The advantages of sulphides over oxides are those the former possess 100 times more electronic conductivity due to smaller band gap. Also due to the lesser electronegativity of sulphur than oxygen, the elongation between the layers occurs which prevent it from structural disintegration and makes the electron transport within the structure easy. The above electrochemical result is proof of advantage for the same.

3.4 Nickel Cobalt Sulphide (NCS-DI)

3.4.1 Material Characterization

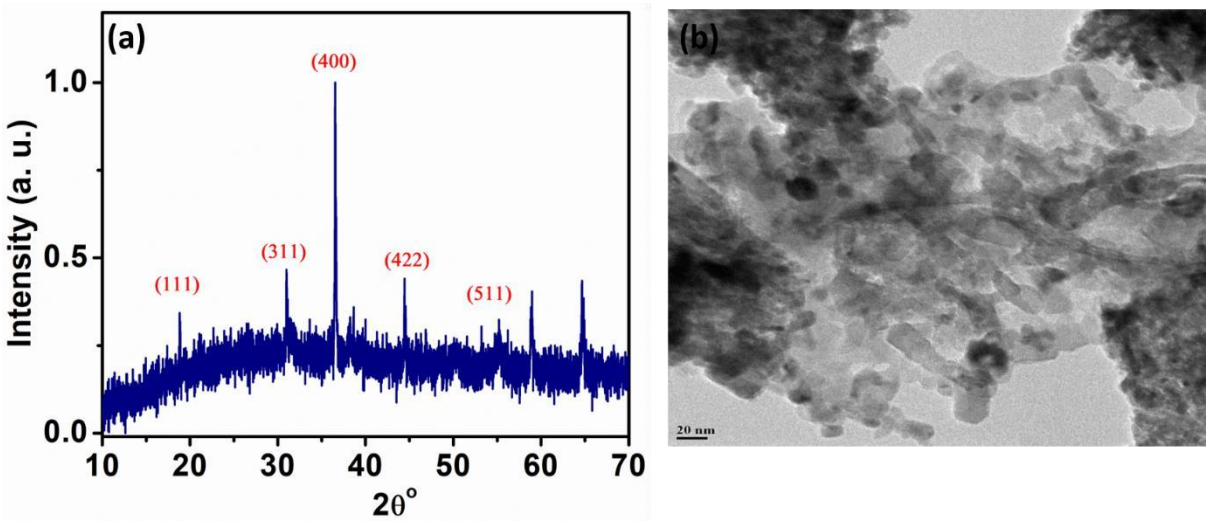

Figure 3.11 (a) XRD marking of NCS-DI and (b) TEM images of NCS-DI at 20nm

The crystal phases of both the materials were examined by XRD as shown in Fig 3.11. In reference with the JCPDS card number # 43-1477, the peaks indexed as (111) (311), (400), (511), (422) correspond to angles 20º, 26.7º, 31.6º, 36.4º, 45.5º and 55.3º respectively. The additional peaks observed may be due to partial remnant $NiCo_2O_4$.

TEM pictures give an instinctive method to explore that few (fig.3.13) are changed over into needle-like structure.

3.4.2 Electrochemical Characterization

The capacitive properties of the NCS-DI are tested the same as above in NCS-1. The system is fixed at 0 to 0.6V potential window for CV and GCD. The cyclic voltammetry measurements were conducted at various sweep rates. In the CV curve. The peak follows the following reactions:

$$\mathbf{NiCo_2S_4 + OH- + H_2O \leftrightarrow NiSOH + 2CoSOH + 2e-}$$

$$\mathbf{CoSOH + OH- \leftrightarrow CoSO + H_2O + e-}$$

$$\mathbf{CoSO + OH- \leftrightarrow CoS_2 + H_2O + e-}$$

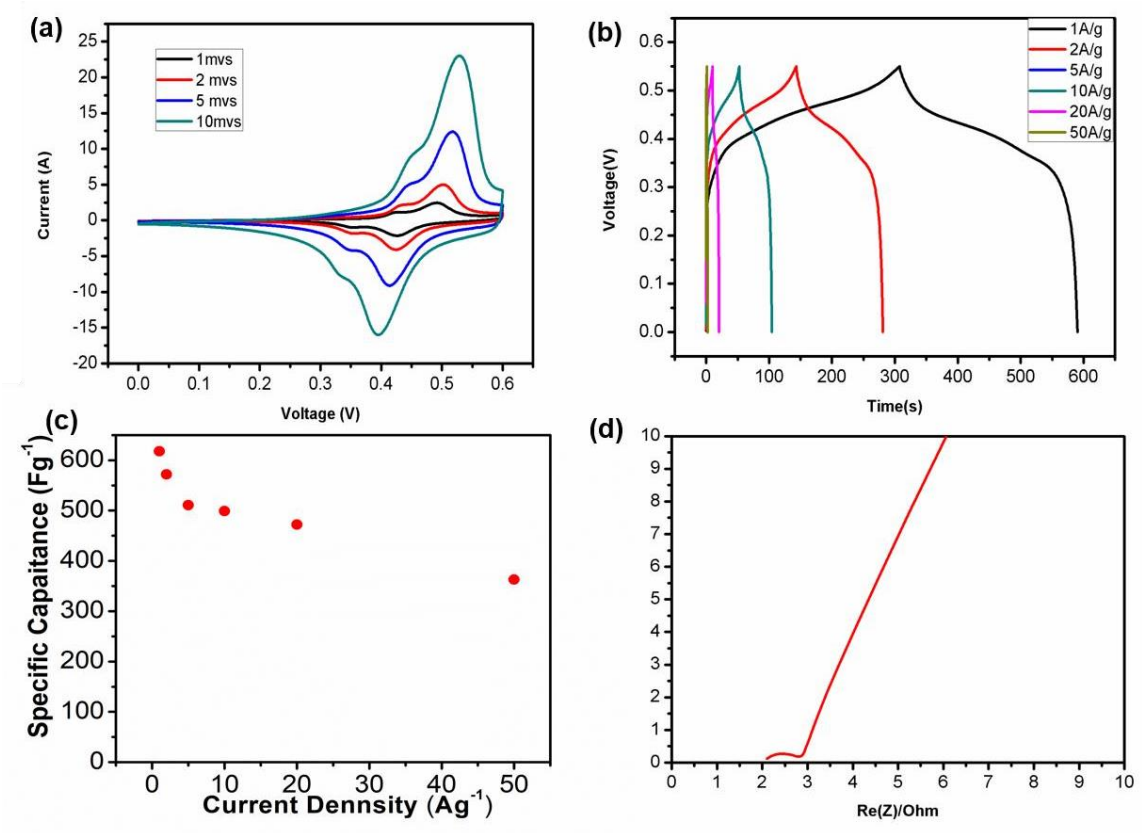

Figure3.12 NCS-DI curves (a) CV curve at several scan rates (b) Charge-Discharge curves at several current densities (c) Rate Capability scatter plot (d) Nyquist graph

In CV curve it is visible it has two peaks in oxidation and two in reduction. The reason for the two peaks is probably due to the presence of both sulphide and oxide phase in NCS-DI material. Capacitance calculated from CD curve at 1A/g, 2A/g, 5A/g, 10A/g, 20A/g is618F/g,569F/g, 530.9F/g, 500F/g, 472F/g, and 363F/g, respectively. In rate Capacity curve the retention of material is greater than 70% for 1A/g to 50 A/g. In EIS there is an internal resistance of 2Ω and R_{ct} 0.9Ω in Nyquist plot and after the semi-circularpart, it shows some resistive behaviour in the diffusive region.

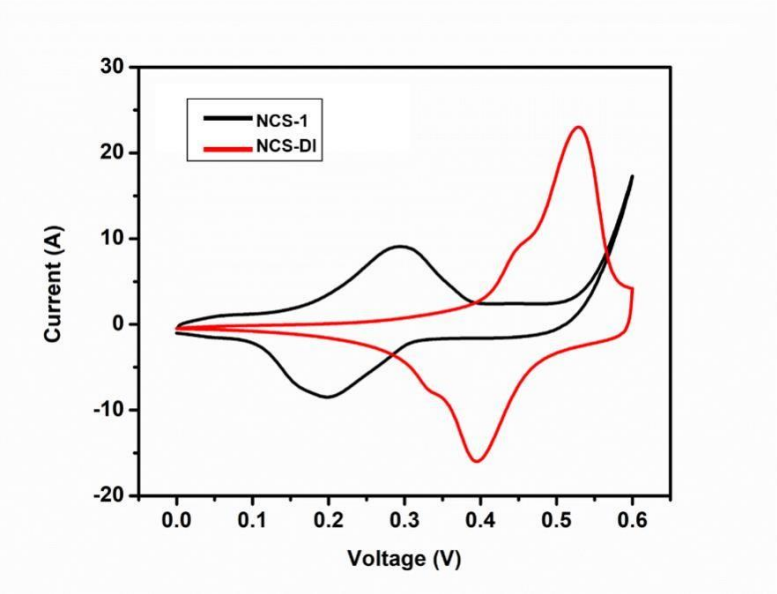

Figure 3.13 CV curves of NCS-DI and NCS-1 at scan rate of 10mVs

In comparison with the NCS-1 electrode, the NCS-DI electrodes exhibit larger integral in CV curves (Fig. 3.13), indicating the NCS-DI electrodes possess higher specific capacitances. Since one step method is more efficient than two-step because it is time convenient as it is done in one step. In comparison with the two-stepmethod, we have to depend on our precursor for the next step. This one-step process is more efficient than the two-step process.

3.5 Nickel Cobalt Sulphide (NCS-EG)

3.5.1 Material Characterization

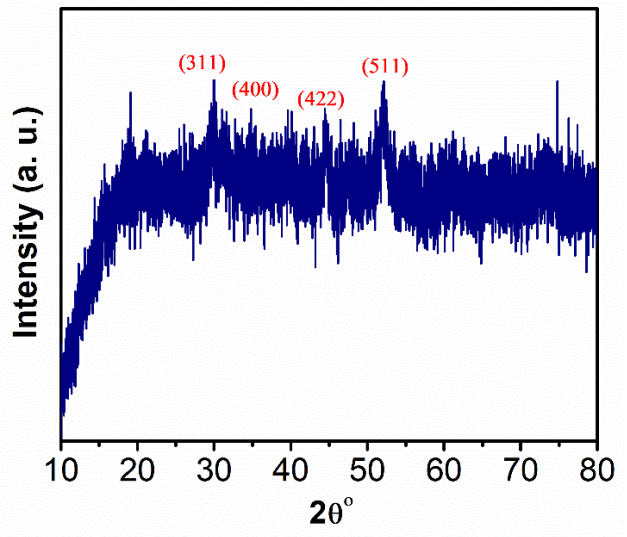

Figure 3.14 XRD marking of NCS-EG

The crystal phases of both the materials were examined by XRD as shown in Figure 3.14. In reference with the JCPDS card number # 43-1477, the peaks indexed as (311), (400), (511) and (422) correspond to angles 28.7º, 32.6º, 54.4º, and 45.3º respectively.

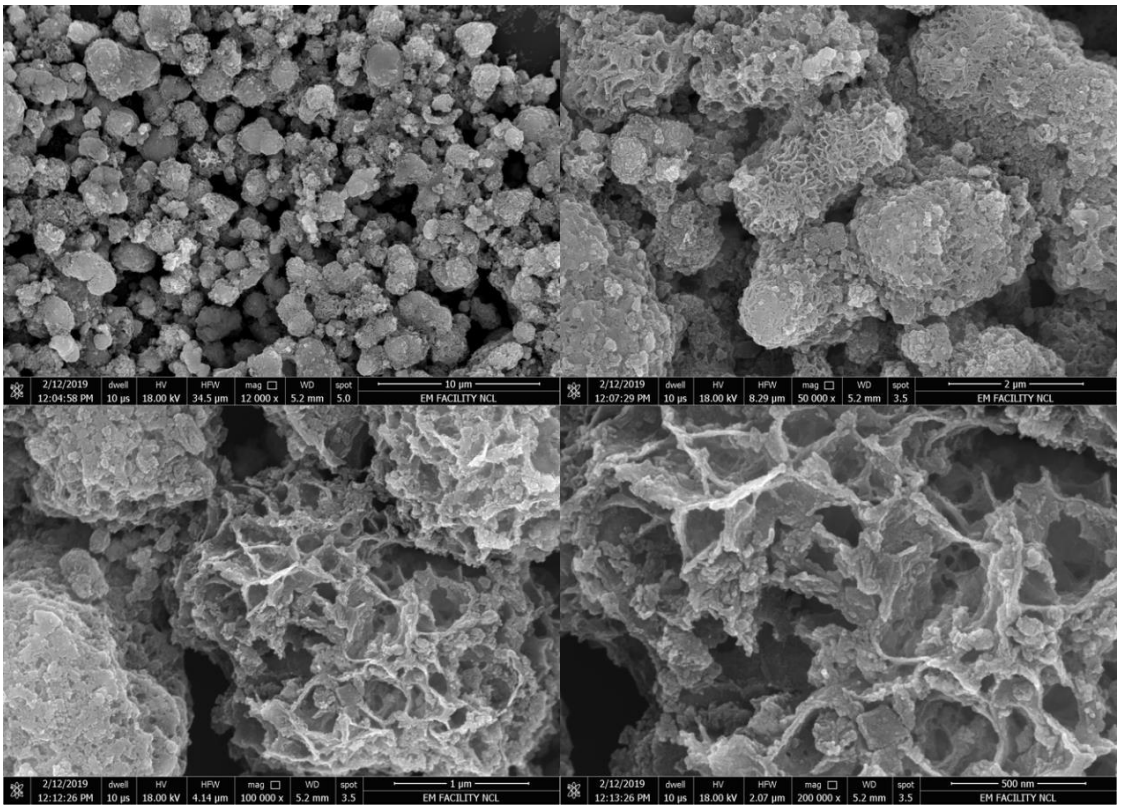

Figure3.15 SEM images of NCS-EG at several nanoscale

The grain size and surface morphology were seen in the Scanning electron microscopy instrument (SEM). SEM pictures of the NCS-EG indicates micron measured particles comprise with permeable system that takes after a loose sponge like structure as appeared in Figure 3.15, the example comprises of nanoscale agglomerates and displays a 3D consistent system structure containing numerous pores with various widths.

3.5.2 Electrochemical Characterization

The capacitive properties of the NCS-EG are tested the same as above in NCS-DI. The system is fixed at 0 to 0.45V potential window for CV and GCD. The cyclic voltammetric measurements were conducted at different scan rates. In the CV curve it is visible NCS has one peak in oxidation and one peak in reduction.

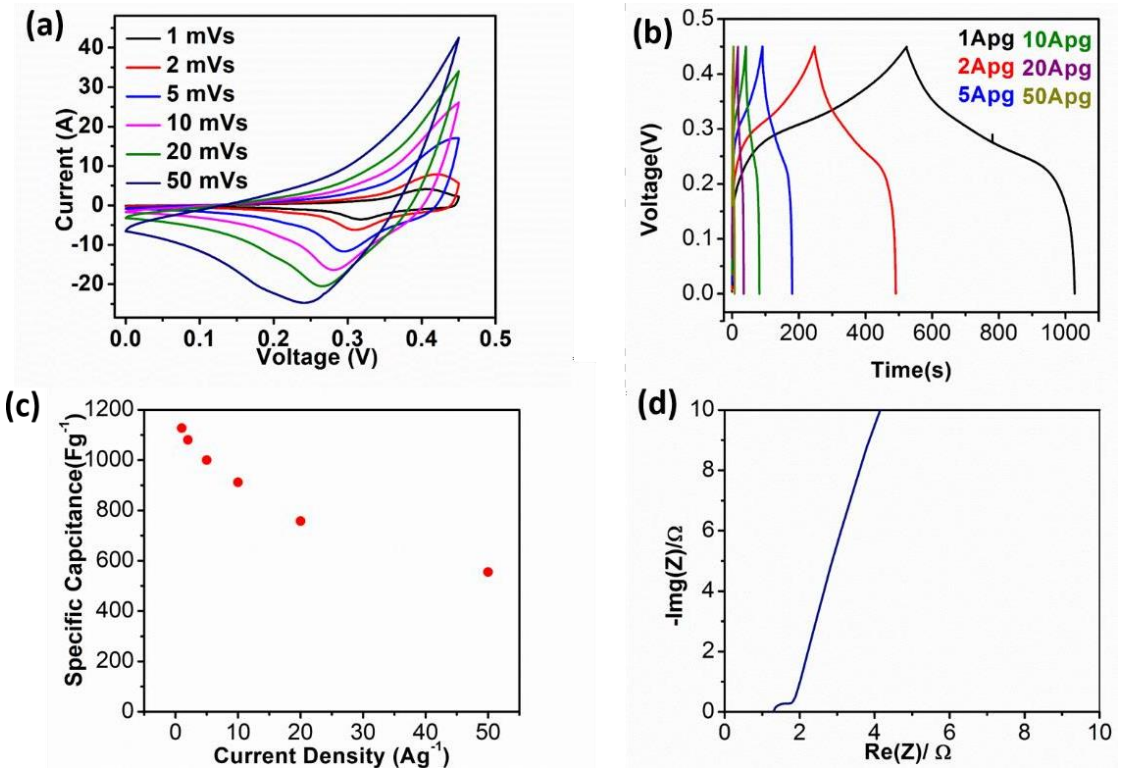

Figure3.16 NCS-EG curves (a) CV curve at several scan rates (b) Charge-Discharge curves at several current densities (c) Rate Capability scatter plot (d) Nyquist graph

Capacitance calculated from CD curve at 1A/g, 2A/g, 5A/g, 10A/g, 20A/g is 1127.4F/g, 1080F/g, 1000F/g, 911.58F/g, 757.57 F/g, and 555.5F/g, respectively. In rate Capacity curve the retention of material is greater than 68% for 1A/g to 50 A/g. In EIS there is an internal resistance of 1.6Ω and R_{ct} is 0.65Ω in Nyquist plot and after the semi-circularpart, it shows some resistive behaviour in the diffusion region.

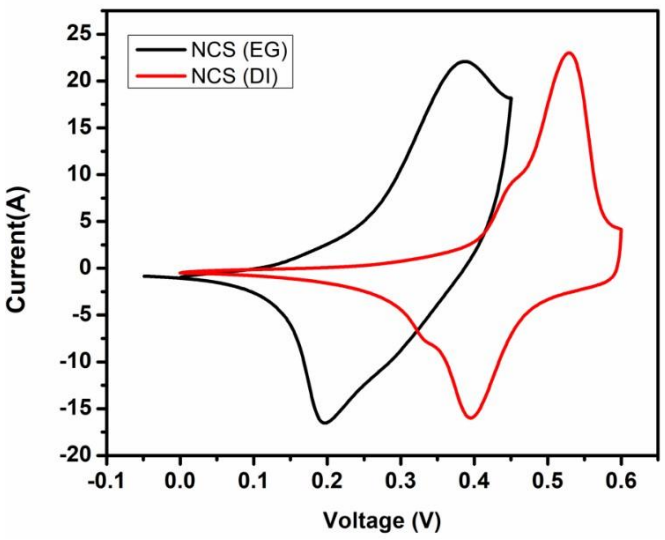

Figure 3.17 CV curves of NCS-DI and NCS-EG at scan rate of 10mVs

In comparison with the NCS-DI electrode, the NCS-EG electrodes exhibit large integral of CV curves (Fig. 3.17), indicating the NCS-EG electrodes possess higher specific capacitances. The dissolvable plays a significant job in the nucleation-development instrument as in aqueous strategy the morphology (SEM characterisation) we got is nanoparticles blended with nanosheets yet in the solvothermal method, we got uniform nanoparticles and it is permeable which perhaps one more purpose for more noteworthy capacitance.

3.6 rGO/Nickel Cobalt Sulphide

3.6.1 Material Characterization

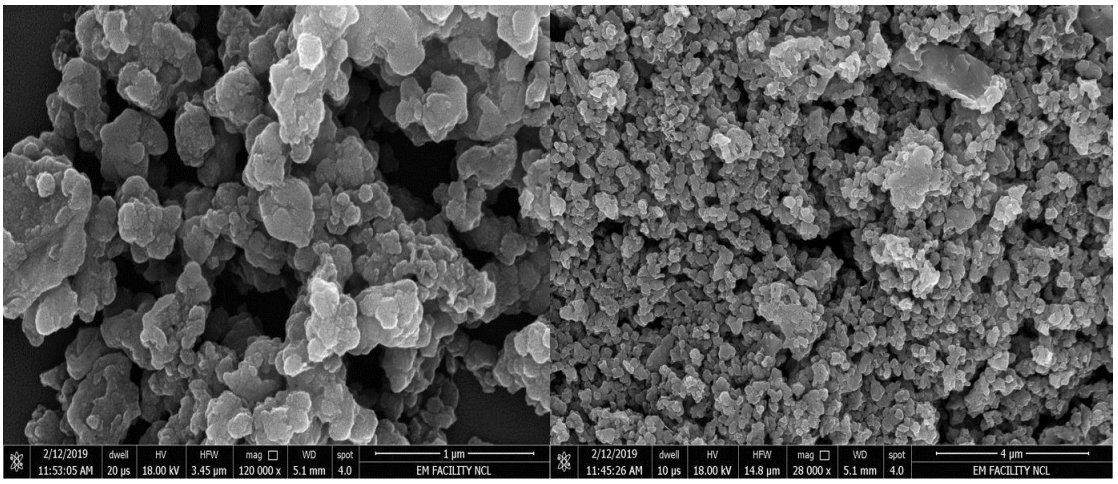

Figure 3.18 SEM images of rGO/NCS at 1µm and 4µm

3.6.2 Electrochemical Characterization

The capacitive properties of the rGO/NCS are tested with the same configuration as in previous electrochemical performance in NCS-EG by one step solvothermal method. The system is fixed at 0 to 0.45V potential window for CV and GCD. The cyclic voltammetric measurements were conducted at different scan rates. In CV plot it has one peak in oxidation and one top in reduction. With the increase of output rate, the potential of the oxidation peak and reduction peak move to the positive andthe negative headings, separately.

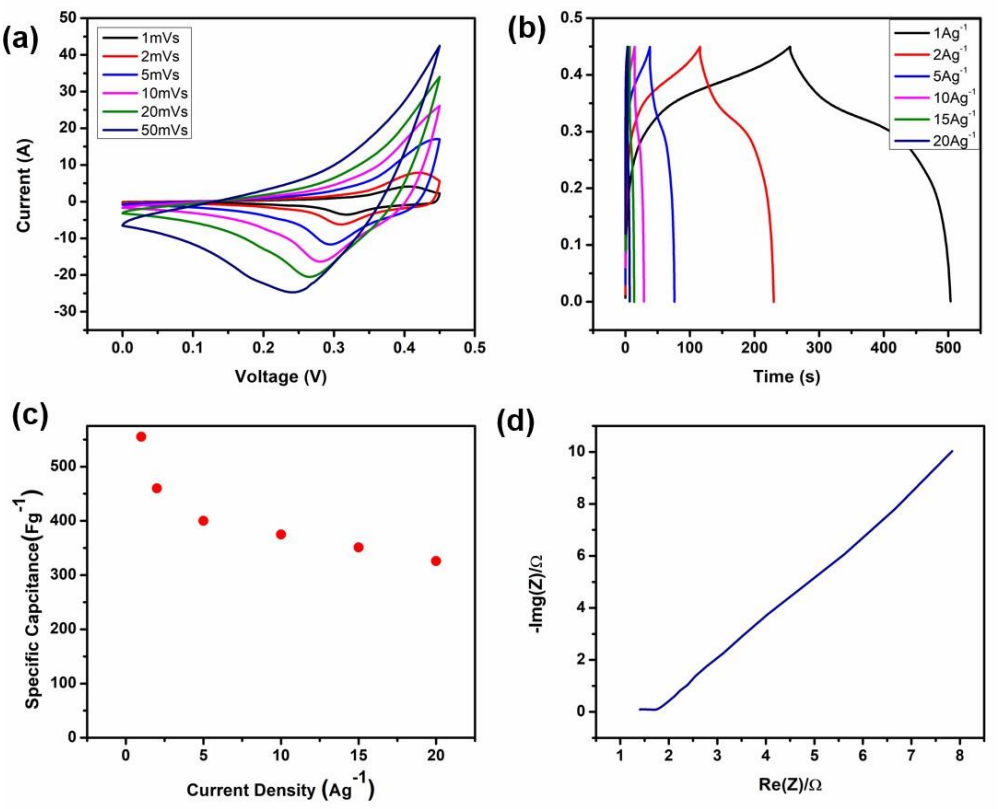

Figure3.19 rGO/NCS curves (a) CV curve at several scan rates (b) Charge-Discharge curves at several current densities (c) Rate Capability scatter plot (d) Nyquist graph

Capacitance calculated from CD curve at 1 A/g, 2 A/g, 5 A/g, 10 A/g, 15 A/g and 20 A/g is 555.5 F/g, 460.33 F/g, 400 F/g, 375.25 F/g, 351.1 F/g, and 326.6 F/g, respectively. In rate Capacity bend the maintenance of material is more noteworthy than 68% for 1A/g to 20 A/g. A major semi-arc implies a bigger obstruction of electrochemical response among electrode and electrolyte. In light of the EIS information, it is discovered that the fitting Rct (0.64 ohms) of rGO/NCS electrode, more vertical line in the low-frequency zone, proposing a progressively perfect capacitive conduct.

Clearly, rGO/NCS electrodes display relatively lower capacitances than every other NCS synthesis and rGO electrode however with phenomenal steadiness because of synergistic impact among NCS and rGO. With the rGO support, electron conduction ways can be made and therefore the solidness and conductivity of rGO/NCS hybrids are incredibly improved, which encourages the charge exchange and charge

transport during the redox process. Additionally, rGO can go about as a viable network for the uniform scattering of the NCS nanoparticles, preventing the total of NCS nanoparticles, and in this way successfully advances the reaction between the electrolyte and the material. Thusly, rGO in NCS/rGO hybrids fills in as both conductive channel and a perfect support network.

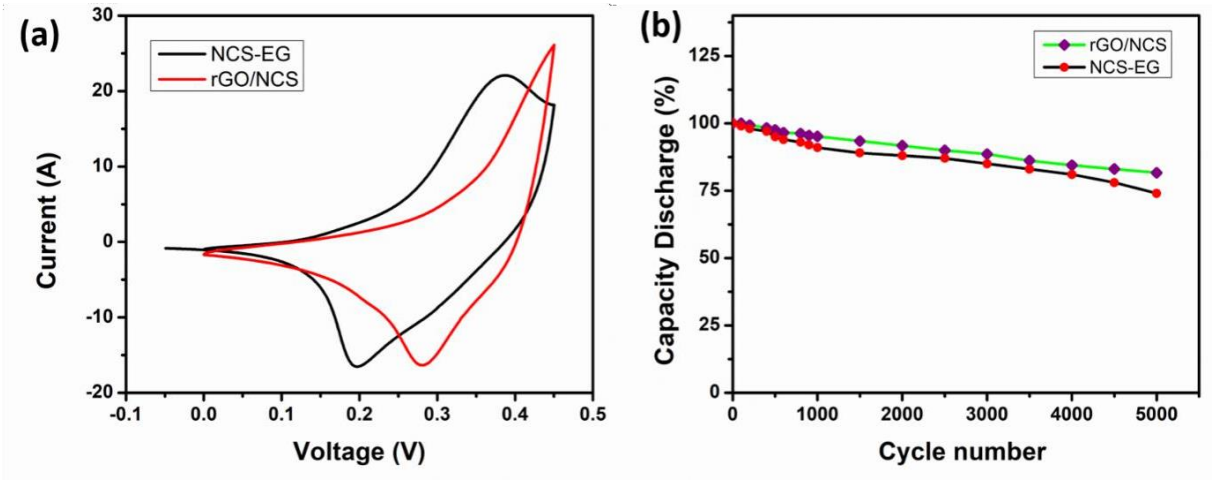

Figure3.20 (a) CV curves of NCS-EG and rGO/NCS at 10mVs scan rate and (b) Stability of NCS-EG and rGO/NCS at current density of $10Ag^{-1}$

The steadiness scattering and line curve demonstrates NCS-EG is more steady than rGO/NCS. Furthermore, the ideal specific capacitance can be acquired through altering the mass ratio of NCS and rGO as the addition of specific capacitance can be credited to the increased substance of active material (NCS) for capacitance age. In any case, the increased substance of NCS will in like manner lessen the substance of GO prompting the reduction of the mechanical steadiness during cycling and increased substance of GO decline the conductivity. In this manner, a reasonable substance of NCS in rGO/NCS crossovers is basic to acquire the ideal electrochemical execution.

Conclusion

In conclusion, the Graphene is synthesised via Modified Hummer's method which shows well defined rectangular CV curve and the symmetrical triangle curve in CD. The specific capacitance obtained at current density of 1 Ag^{-1} is 78 Fg^{-1}, excellent rate capability with specific capacitance 58.8 Fg^{-1} at 50 Ag^{-1} with 78% of initial capacitance retention. Next comes the synthesis of NCO via hydrothermal method with two different nucleation rate named as NCO-r_1 and NCO-r_2.

NCO-r_1 gives better performance compared to NCO-r_2 which act as precursor for NCS-1 and shows good specific capacitance than NCO-r_1. NCS were synthesised by three different methods and their specific capacitance at current density of 1 Ag^{-1} is 366.6 Fg^{-1} (NCS-1), 618 Fg^{-1} (NCS-DI) and 1127.4 Fg^{-1} (NCS-EG) in which NCS-EG by Solvothermal method shows excellent specific capacitance of 1127 Fg^{-1} at current density of 1 Ag^{-1} with 68% retention from 1Ag^{-1} to 50 Ag^{-1} compared to initial capacitance. The composite of NCS with graphene was successfully synthesised and gives specific capacitance of 555.5 Fg^{-1} at current density of 1 $Ag^{-}1$ and it shows excellent result among the synthesised potential electrode materials. The performance can be improved further through optimization of loading of Graphene and NCS. The easy union and amazing electrochemical property of the NCS/rGO hybrids make them promising electrode materials for supercapacitor application.

References

1. Mourad, E.; Coustan, L.; Lannelongue, P.; Zigah, D.; Mehdi, A.; Vioux, A.; Freunberger, S. A.; Favier, F.; Fontaine, O. Biredox Ionic Liquids with Solid-like Redox Density in the Liquid State for High-Energy Supercapacitors. *Nat. Mater.* **2016**, *16* (November 2016).
2. Kumar, A., Kumar, K., Kaushik, N., Sharma, S., & Mishra, S. (2010). Renewable energy in India: current status and future potentials. *Renewable and sustainable energy reviews*, *14*(8), 2434-2442.
3. Wang, S., Wei, T., & Qi, Z. (1008). Supercapacitor energy storage technology and its application in renewable energy power generation system. In *Proceedings of ISES World Congress 1007 (Vol. I–Vol. V)* (pp. 2805-2809). Springer, Berlin, Heidelberg.
4. Principle, T. W.; Cell, S. The Working Principle of a Solar Cell. **1921**, *1*, 21–24.
5. Characteristics, C. Chapter 2 Electrode / Electrol Yte Interfaces: Structure and. **1900**.
6. https://www.explainthatstuff.com/how-supercapacitors-work.html
7. Enrique Herrero, Lisa J. Buller, Héctor D. Abruña, Underpotential Deposition at Single Crystal Surfaces of Au, Pt, Ag and Other Materials, Chem. Rev. 101 (7) (1001) 1897–1930.
8. Jiang, J., Zhang, Y., Nie, P., Xu, G., Shi, M., Wang, J.,& Zhang, X. (2018). Progress of nanostructured electrode materials for supercapacitors. *Advanced Sustainable Systems*, *2*(1), 1700110.
9. Veronica Augustyn, Patrice Simon, Bruce Dunn, Pseudocapacitive Oxide Materials for High-rate Electrochemical Energy Storage, Energy Environ. Sci. 7 (5) (2014) 1597-1614.
10. Arkady A. Karyakin, Prussian blue and Its Analogues: Electrochemistry and Analytical Applications, Electroanalysis 13 (10) (1001) 813-819.
11. Venkataraman, A. (2015). Pseudocapacitors for Energy Storage.
12. Simon, P., & Gogotsi, Y. (2010). Materials for electrochemical capacitors. In *Nanoscience and Technology: A Collection of Reviews from Nature Journals* (pp. 320-329).

13. Largeot, C., Portet, C., Chmiola, J., Taberna, P. L., Gogotsi, Y., & Simon, P. (1008). Relation between the ion size and pore size for an electric double-layer capacitor. *Journal of the American Chemical Society*, *130*(9), 2730-2731.
14. Chidembo, A. T., Ozoemena, K. I., Agboola, B. O., Gupta, V., Wildgoose, G. G., & Compton, R. G. (2010). Nickel (II) tetra-aminophthalocyanine modified MWCNTs as potential nanocomposite materials for the development of supercapacitors. *Energy & Environmental Science*, *3*(2), 228-236.
15. Bello, A., Makgopa, K., Fabiane, M., Dodoo-Ahrin, D., Ozoemena, K. I., & Manyala, N. (2013). Chemical adsorption of NiO nanostructures on nickel foam-graphene for supercapacitor applications. *Journal of materials science*, *48*(19), 6707-6712.
16. Jafta, C. J., Nkosi, F., le Roux, L., Mathe, M. K., Kebede, M., Makgopa, K., & Chen, S. (2013). Manganese oxide/graphene oxide composites for high-energy aqueous asymmetric electrochemical capacitors. *Electrochimica Acta*, *110*, 228-233.
17. Frackowiak, E. (1007). Carbon materials for supercapacitor application. *Physical chemistry chemical physics*, *9*(15), 1774-1785.
18. Lai, C. H., Lu, M. Y. & Chen, L. J. Metal sulfide nanostructures: synthesis, properties and applications in energy conversion and storage. J. Mater. Chem. 22, 19–30 (2012).
19. Li, L. et al. Single-crystalline CdS nanobelts for excellent field-emitters and ultrahigh quantum-efficiency photodetectors. Adv. Mater. 22, 3161–3165 (2010).
20. Radovanovic, P. V., Barrelet, C. J., Gradecak, S., Qian, F. & Lieber, C. M. General synthesis of manganese-doped II-VI and III-V semiconductor nanowires. Nano Lett. 5, 1407–1411 (1005).
21. Fang, X. S. et al. Single-crystalline ZnS Nanobelts as ultraviolet-light sensors. Adv. Mater. 21, 2034–2039 (1009).
22. Xiong, S. L. & Zeng, H. C. Serial ionic exchange for the synthesis of multishelled copper sulfide hollow spheres. Angew. Chem. Int. Ed. 51, 949–952 (2012)
23. Chen, H. C. et al. Highly conductive $NiCo_2S_4$ urchin-like nanostructures for high-rate pseudocapacitors. Nanoscale 5, 8879–8883 (2013).

24. Yu, L., Zhang, L., Wu, H. B. & Lou, X. W. Formation of $Ni_xCo_{3-x}S_4$ hollow nanoprisms with enhanced pseudocapacitive properties. Angew. Chem. Int. Ed. 53, 3711–3714 (2014).
25. Pu, J. et al. Direct growth of $NiCo_2S_4$ nanotube arrays on nickel foam as high performance binder-free electrodes for supercapacitors. Chempluschem 79, 577–583 (2014).
26. Chen, W., Xia, C. & Alshareef, H. N. One-step electrodeposited nickel cobalt sulfide nanosheet arrays for high-performance asymmetric supercapacitors.ACS Nano 8, 9531–9541 (2014).
27. Long JW, Swider KE, Merzbacher CI et al. Voltammetric characterization of rutheniumoxide-based aerogels and other RuO_2 solids: the nature of capacitance in nanostructuredmaterials. Langmuir 1999; 15:780–5.
28. Hu C-C, Chen W-C,Chang K-H.How to achieve maximum utilization of hydrousruthenium oxide for supercapacitors. J Electrochem Soc 1004; 151:A281–90
29. Wu, H. Y., & Wang, H. W. (2012). Electrochemical synthesis of nickel oxide nanoparticulate films on nickel foils for high-performance electrode materials of supercapacitors. *Int. J. Electrochem. Sci*, *7*, 4405-4417.
30. S. Wang, J. Pu, Y. Tong, Y. Cheng, Y. Gao, Z. Wang, $ZnCo_2O_4$ nanowire arrays grown on nickel foam for high-performance pseudocapacitors, J. Mater. Chem. A 2(2014) 5434.
31. K. Xu, J. Yang, J. Hu, Synthesis of hollow $NiCo_2O_4$ nanospheres with large specific surface area for asymmetric supercapacitors, Journal of Colloid and Interface Science (2017)
32. Wang, H. L.; Gao, Q. M.; Jiang, L. Small. Facile approach to prepare nickel cobaltitenanowire materials for supercapacitors.2011, 7, 2454.
33. Jiang, H.; Ma, J.; Li, C. Z. Chem. Commun. Hierarchical porous $NiCo_2O_4$ nanowires for high-rate supercapacitors. 2012, 48, 4465.
34. Fei-Xiang Ma, Le Yu,Cheng-Yan Xu and Xiong Wen (David) Lou. Self-supportedformation of hierarchical NiCo2O4 tetragonal microtubes with enhancedelectrochemical properties. Energy Environ. Sci., 2016, 9, 862
35. Qiufan Wang, Bin Liu, Xianfu Wang, Sihan Ran, Liming Wang, Di Chen and GuozhenShen. Morphology evolution of urchin-like $NiCo_2O_4$ nanostructures

and theirapplications as psuedocapacitors and photoelectrochemical cells. J. Mater. Chem., 2012, 22, 21647

36. Pu, J. et al. Preparation and electrochemical characterization of hollow hexagonal $NiCo_2S_4$ nanoplates as pseudocapacitor materials. ACS Sustainable Chem. Eng. 2, 809–815 (2014).
37. Peng, S. J. et al. In situ growth of $NiCo_2S_4$ nanosheets on graphene for highperformance supercapacitors. Chem. Commun. 49, 10178–10180 (2013)
38. Scrosati, B. (1989). Conducting polymers and their applications. In *Materials Science Forum* (Vol. 42, pp. 207-220). Trans Tech Publications
39. Na, G. U. O., Yanhua, L. E. I., Tao, L. I. U., & Xueting CHANG, Y. Y. (2018). Electrochemical Deposition of Polypyrrole Coating on Copper from Aqueous Phytate Solution and Its Application in Corrosion Protection. *Journal of Chinese Society for Corrosion and protection*, *38*(2), 140-146
40. Jha, P. K., Singh, S. K., Kumar, V., Rana, S., Kurungot, S., & Ballav, N. (2017). High-Level Supercapacitive Performance of Chemically Reduced Graphene Oxide. *Chem*, *3*(5), 846-860.